38th International Electric Vehicle Symposium and Exhibition (EVS38) Göteborg, Sweden, June 15-18, 2025

Evaluating the Potential of Sodium-Ion Batteries for Low Voltage Mobility

Karsten Mueller[1], Sébastien Sallard[2], Brahim Soltani[2], Alexander Fandakov[1], Johannes Werfel[1], Marc Sens[1]

[1] *IAV GmbH, Carnotstr. 1, 10587 Berlin, Germany, karsten.mueller@iav.de*
[2] *IAV France S.A.S., 4 rue Georges Guynemer, 78280 Guyancourt, France*
Correspondence: karsten.mueller@iav.de

Executive Summary

The automotive industry is under pressure to reduce greenhouse gas emissions. While the growth of electric vehicles (EV) is crucial, optimizing low-voltage batteries for conventional powertrain architecture (12V-48V) can help reduce carbon dioxide (CO2) emissions. Currently, Lithium Iron Phosphate (LFP) batteries dominate the low voltage battery market due to their stability, safety, and ecological benefits as replacement to lead-acid (Pb-A). However, Sodium-Ion Batteries (SIB) are emerging as a promising alternative to LFP, offering advantages in power, lifespan, cold temperature performance, integration, cost, material availability, and sustainability. These advantages of sodium-ion batteries make them a perfect candidate for fulfilling the requirements typically associated with 48V applications as well. This contribution evaluates low-voltage SIB prototypes developed by IAV and its partners and explores their potential for automotive applications, aiming to share insights and assess future prospects.

Keywords: sodium-ion, lithium-ion, low-voltage, battery system, hybrid

1 Introduction

Within the transport sector, the imperative to limit global warming emissions is driving the automotive industry to reduce the amount of greenhouse gases. In anticipation of the 2035 ban on internal combustion engine (ICE) vehicles, the European Union (EU) mandates a continuous reduction in CO_2 emissions from new vehicles fleets sold within its jurisdiction [1]. However, the recent slowdown in electric vehicle (EV) adoption across the EU poses a challenge to achieving these targets [2]. Enhancing the performance of low-voltage batteries - whether the 12V batteries for onboard networks or the 48V batteries in Mild Hybrid Electric Vehicles (mHEV) - offers significant benefits in terms of performance and energy savings, ultimately contributing to the overall reduction of CO_2 emissions in the vehicle fleet.

1.1 State of the Art in 12V Applications

In recent years, the automotive industry has witnessed a growing interest in transitioning from traditional lead-acid 12 V batteries to alternative technologies, primarily driven by concerns over the toxicity of lead and the anticipation of potential future bans. This shift necessitates a comprehensive analysis of the relevance and implications across a handful critical areas including strategy and supply chain, environmental impact, economics, and performance. Among the promising alternatives to lead-acid, especially the lithium-ion technology has emerged as a viable option as discussed in the following sections, also implying changes to the overall system by necessitating the inclusion of a battery management system.

1.1.1 Lead acid batteries

For automotive 12V applications, lead-acid batteries are the most commonly used battery technology. These batteries typically consist of 6 cells connected in series, with each cell having a voltage of approx. 2.0 V, delivering a voltage of 12 V. The main reason for the historical dominance of the lead acid battery use, especially for ICE vehicles, is its low cost combined with the ability to deliver high discharge currents at low temperatures with a typical starting current ranging from hundreds to even thousands of amperes. The disadvantages of the Pb-A battery technology are a limited lifetime, especially at high depth of discharges (DoD), and a low energy density, usually close to 50 Wh/kg [11, 12].

1.1.2 NMC batteries

Nickel-manganese-cobalt (NMC) technology employs nickel-manganese-cobalt oxides $LiNi_xMn_yCo_zO_2$, introduced in 2001, as cathodic material. The original chemistry was x = y = z = 1/3 also known as NMC 111 or stoichiometric NMC. Later NMC with high nickel-content, Ni-rich NMCs, have emerged from 532 to 622 and 811 and even beyond. The higher the nickel-content of the NMC material the bigger its specific practical capacity, from 153 mAh/g for the NMC111 to 198 mAh/g for the NMC811, and thus the energy density has increased significantly by ca. 15% [5]. Nowadays NMC-cells show the highest energy density due to their high capacity and high voltage (mean voltage at 3.7 V), Figure 1, a value of 250 Wh/kg can be considered common. Energy density values close to 300 Wh/kg at cell level are already available. In addition, increasing the nickel content of the NMC material increases the cell power. Another advantage of Ni-rich NMCs is their limited cost and ecological impact due to low cobalt content. However, the cobalt element is a stabilizer for the NMC, lower the cobalt content, the faster the capacity fades and easier its thermal degradation, i.e. and more dramatic the thermal runaway of the NMC cells. Last but not least, the economic viability of LIB cell recycling is highly dependent on the valuable materials in, mostly its cobalt content.

1.1.3 LFP batteries

Lithium iron phosphate $LifePO_4$, a olivine-type mineral, was first reported as a cathodic material for LIBs in 1996. LFP batteries are advantageously cobalt-free, i.e. cheaper and more sustainable than NMC-based (nickel manganese cobalt oxide) batteries. LFP is a stable cathodic material, especially when compared to standard layered metal oxides $LiMO_2$ (M = transition metal element) such as NMC and LMO (lithium manganese oxide). Thus, LFP-based batteries present an extended lifetime and are considered safer than the other Li-ion batteries [13, 14]. The LFP material shows poor electronic conductivity which is critical for the performance of the LFP-based batteries. To mitigate this limitation, commercial LFP materials are normally covered by a thin and conductive carbon coating. The LFP material is also occasionally labelled as LFP/C. The energy density of LFP batteries is dependent on their design. In an energy-type configuration, 200 Wh/kg has already been reached at cell level [4]. Higher values have even been recently announced presently (230 Wh/kg). High energy LFP cells have a limited discharge rate, usually 3C to 5C for the best.

Power-type cells can reach more than 3 kW/kg (60 C discharge rate) combined with limited energy density, usually close to 80-90 Wh/kg [15, 16]. Low cost, combined with reasonable energy density and good safety makes the LFP-cells as a “rising” star in the last year to power most of the new EVs while the NMC-cells are used within premium and long driving range vehicles [17]. As already mentioned, LFP is cobalt-free thus usually considered to be more environmentally friendly than NMC cells, but the recycling of the former is presently not economically viable contrary to the latter.

1.1.4 LTO cells

Still being a niche market, lithium titanate oxide (LTO) cells use $Li_4Ti_5O_{12}$ as anode material. The LTO cells offer high power and high stability. The LTO cells can intuitively be considered safer than other LIBs, the LTO anode has a medium voltage, compatible with the standard carbonate electrolyte. The fragility of the solid electrolyte interphase (SEI) is much less critical in comparison to standard cells using graphitic anodes. Consequently, the thermal runaway scenario initiated by self-warming of the cell [C] is much less at risk to happen. LTO cells suffer from a limited energy density, ca. 50 Wh/kg, due to their low mean voltage at 2.4 V (Figure 1) and the limited capacity of the LTO anode [18]. The LTO-cells also suffer from high costs and are not cobalt free, i.e. hardly sustainable, due to their NMC-based cathode [7].

1.1.5 State of the art

In the low voltage battery segment, among the different Li-ion battery technologies, LFP is considered as one of the best candidates [3]. For certain low voltage applications like 12V, LFP is already replacing Pb-A [3]. Environmental low temperatures, below 0°C, lead to reversible decrease of the performances of the Li-ion batteries as it is expected for all chemical reactions and it is described by the (Arrhenius equation) [L]. It is mostly attributed to the drop of the ionic conductivity of the electrolyte and the rise of the charge transfer resistance between the electrolyte and the electrodes, i.e. the transport of the Li-ions through the cathode electrolyte interphase (CEI) and solid electrolyte interphase (SEI) and the Li-ion desolvation before insertion in the solid active material [19, 20, 21]. Note that low temperatures can also lead to irreversible degradation during cell cycling, especially during fast charging but it is not the topic of this article. . LFP technology is even more sensitive to cold temperatures than the other LIB technologies due to its high energy activation Ea (Arrhenius equation) and the limited 1D ion transport mode of the LFP material [19, 22]. Last but not least the SoC evaluation of LFP batteries is complex and cannot rely on the measured voltage (Figure 1), inducing supplementary costs for an accurate battery management system [23].

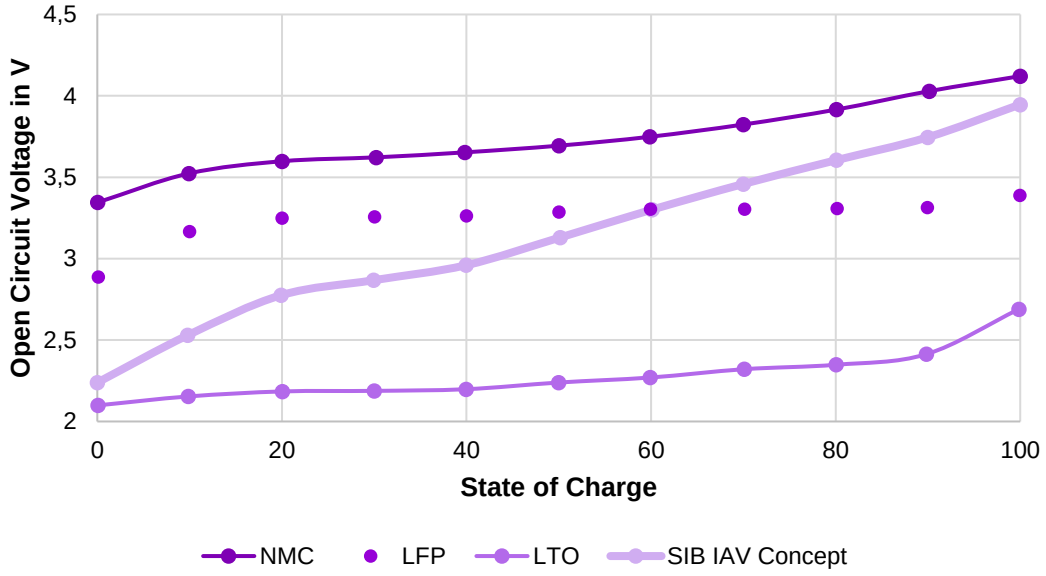

Figure 1: Comparison of open circuit voltage of different LIB and SIB over state of charge.

1.2 State of the Art in in 48V Applications

Mild hybrid vehicles are a promising technology for reducing CO_2 emissions in the near term. This architecture includes an electric machine alongside a conventional internal combustion engine to improve efficiency and reduce emissions thanks to the application of a 48 V system. There are different variant architectures of these systems, influencing their performance and cost-effectiveness. First, we explore the different architectures of mild hybrid systems in the following section, focusing on their configurations, benefits, and limitations.

1.2.1 48 V in Mild Hybrid Vehicles

The **P0 architecture** is the simplest form of mild hybridization. It involves integrating the electric machine into the front-end accessory drive (FEAD) belt of the ICE, Figure 2. This setup allows for basic functions like engine stop/start and regenerative braking. While it is cost-effective and easy to implement, the P0 architecture suffers from higher friction losses due to the permanent connection between the electric machine and the ICE. This reduces energy recuperation potential and overall efficiency. In the **P1 setup**, the electric machine is connected directly to the crankshaft of the ICE. This allows for improved energy recuperation and engine load shifting, enhancing efficiency. However, like the P0 architecture, the P1 system is limited in its ability to provide pure electric driving and has reduced efficiency due to engine friction.

The **P2 architecture** offers more advanced hybrid functions by decoupling the electric machine from the ICE as shown in Figure 2. It can be mounted coaxially or side-mounted on the transmission. This configuration allows for better energy recuperation, torque assist, and limited pure electric driving. The P2 system improves efficiency by optimizing the operating point of the electric machine and enabling engine downsizing. On the

negative side, the P2 architecture is more complex and costly compared to P0 and P1. The **P3 architecture** places the electric machine on the output side of the transmission. This setup provides high recuperation potential and allows for pure electric driving. It can also enhance vehicle performance through torque assist. However, the P3 system cannot start the ICE and lacks the ability to optimize the electric machine's operating point through variable transmission gear ratios, which limits overall efficiency improvement.

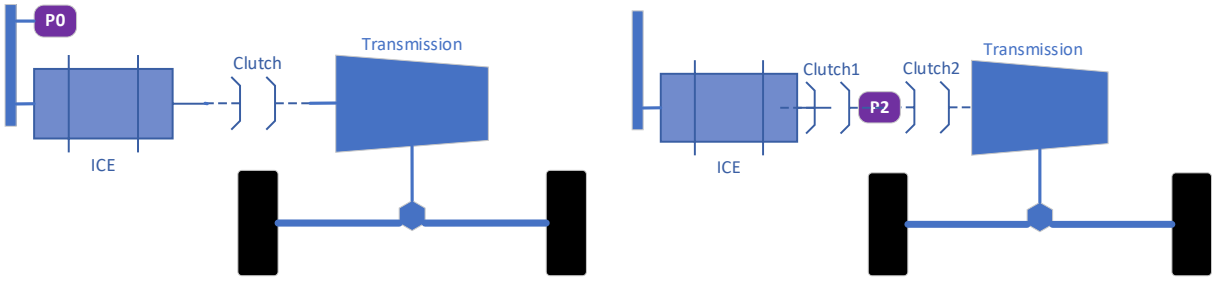

Figure 2: Overview of P0 and P2 mild hybrid powertrain layouts.

In the **P4 configuration**, the electric machine is connected to the rear axle, providing electric all-wheel drive capabilities. This architecture offers high energy recuperation potential and allows for pure electric driving. The P4 system is advantageous for torque vectoring and improved vehicle handling. However, it is more costly due to the additional electric machine. Another disadvantage is the increased unsprung mass, which can affect vehicle dynamics. Finally, the **P5 architecture** is a more advanced version of the P4 system, featuring individual control of non-driven wheels. This setup enhances safety and handling through torque vectoring and individual brake control. While it offers significant benefits in terms of performance, the P5 architecture is expensive and poses safety risks due to uncontrolled yaw moments if one electric machine fails.

The choice of architecture depends on the desired balance between performance and cost-effectiveness. More complex systems like P2, P3, and P4+P0 offer substantial CO_2 reduction and fuel savings, making them attractive options for reducing emissions in the near term. However, simpler architectures like P0 and P1 provide a cost-effective entry point into hybridization, suitable for manufacturers looking to meet stringent CO_2 targets without significant investment.

1.2.2 48 V Application in Electric Vehicles

Beyond hybrid powertrain applications, 48V systems are increasingly gaining attention in fully electric vehicles, with first OEMs having already introduced vehicles equipped with 48V board net systems, such as the Tesla Cybertruck. A fully 48 V-based architecture supplies components like windows, doors, touchscreen and air suspension pumps. Because of its higher voltage, a 48 V system can send the same power with less current, which means less heat, smaller wires, and cheaper, lighter parts. This helps make the system more efficient and cuts down on weight. Alternatively, he implementation of a 48 V system enables a significant increase of the peak power levels and thus the application of technologies not feasible at lower voltages, e.g. steer-by-wire, with the Tesla setup using a handful of motors. The increased voltage level also allows for innovative features like PowerShare (bi-directional charging) and makes the overall electrical system more reliable. Tesla's switch to 48 V in the Cybertruck is a big change for the car industry and helps save costs while making the system simpler and more powerful.

1.2.3 48 V Energy Storage System State of the Art

State-of-the-art 48V battery systems mainly use advanced lithium chemistries. NMC is favored for higher energy and power density, LFP for safety and longevity at lower cost, and LTO for extreme durability and fast charging but at a premium price, as discussed in section 1.1. Mild hybrid 48 V systems often use NMC or LFP due to their balanced performance and cost, while LTO is less common due to expense despite its safety and lifespan advantages. In this context, the application of new chemistries can help address known pain points related to the state of the art, yielding additional benefits.

The optimal 48 V battery system is application-dependent, considering the specific power and energy requirements related to the target vehicle and powertrain (EV or MHEV). Furthermore, mild hybrid architectures vary significantly in complexity, cost, and efficiency. The P2 mild hybrid architecture is

considered to offer better balance between cost, complexity, and efficiency compared to P1 and P3. It improves fuel savings and energy recovery more than P1 by placing the e-motor between engine and transmission, thus reducing losses. While P3 provides slightly better performance, it's more complex and costly. Thus, P2 delivers overall strong efficiency gains with moderate cost and easier integration, making it a popular choice for mild hybrids.

1.3 New chemistries evolving

Sodium-ion batteries (SIBs) have emerged as promising new battery technology in recent years, offering numerous advantages. SIB technology is already reaching an industrial scale with factory production capacities exceeding GWh/year. Its industrial utilization is starting as well in many fields ranging from mobility to stationary applications [6].

SIBs have a similar working principle than other batteries, especially compared to LIBs, during the charge, the active material in the positive electrode is oxidized, i.e. electrons are ejected from it to be collected by the current collector and transported outside the cell via the external electrical circuit. To maintain the neutrality balance, alkali counter ions (Na-ion for SIB, Li-ion for LIB) are extracted from the positive active material and are solvated in the electrolyte at the solid/liquid interface. In same time, the inverse reactions occur on the negative electrode side, i.e. its active material is reduced by the electrons coming from the external circuit (current flow) and solubilized alkali ions from the electrolyte insert in the active negative material after a desolvation step. Reactions are inversed during the discharge. The main difference between SIBs and LIBs is the use as mobile ion of the sodium Na^+ in the former and lithium Li^+ in the latter. This "little" change has important effects. As disadvantages, SIBs present a limited energy density than LIBs, active materials can hardly exchange as many big sodium-ions (diameter = 95 pm) as small Li-ions (diameter = 60 pm). In addition, the standard graphite is not suitable for the storage of Na-ion, the graphite storage of sodium ions is too poor capacity with usual battery electrolyte, ca.3% of the one of graphite with lithium ions. Thus, hard carbon is the most standard anode materials for SIB, its capacity is limited (ca. 300 mAh/g) but its electrochemical behavior is different too. Soft carbon is used by some companies as well. As advantages, the different behavior of the Na-ions in the liquid electrolyte is different from the one of the Li-ion. The former is less affected by cold temperatures as -30°C than the latter. Thus, the slowing down of the electrochemical reaction kinetics occurring in a running SIB is mitigated compared to a LIB, in agreement with limited power loss of SIBs at low temperatures [4, 24, 25].

Like the LIBs, the SIBs is a generic wording which includes different technologies. Three main families can be listed based on their cathodic material, each of them having its pros and cons: Prussian Blue $Fe[Fe(CN)_6]\cdot 6\ H_2O$ (PB) and analogs (PBAs, mostly the Prussian White $Na_xK_yFe_2(CN)_6\cdot z\ H_2O$), layered metal oxides (globally based on the $NaMO_2$ formula) and polyanions (mostly known for the vanadium fluor-phosphate developed by Tiamat $Na_3V_2(PO_4)_2F_3$ NVPF) [26, 27]. Sodium-ion batteries offer good performance at extreme temperatures and fast charging. While they have lower energy density than lithium-ion batteries, their long cycle life, safety, and abundant materials make them attractive for cost-effective and sustainable applications. With these characteristics, sodium-ion technology emerges as an interesting alternative to lithium-ion technology in the context of low-voltage applications. This has motivated the development of sodium-ion-based concepts dedicated to 12 V and 48 V applications by the authors, which are presented in the following section.

2 IAV's Low-Voltage Sodium-Ion Concepts

In 2023, IAV presented a twin high-voltage battery concept combining sodium-ion and lithium-ion solid-state cells. The LIBs offer long driving range while SIBs provide power, efficiency at low temperature and lower the environmental impact sustainability[10]. Along with some partners, IAV has recently focused efforts into developing and evaluating low-voltage SIB prototypes, following interest in this technology for power applications in the automotive industry. The purpose of this section is to share some of the results that we obtained through this project and present the developed dedicated, sodium-ion-based 12 V and 48 V battery module concepts, demonstrating the potential of this technology.

2.1 12 V Sodium-Ion Concept

In 2024, in collaboration with HiNa, IAV presented a 12 V SIB prototype to the public, based on a 7P4S configuration selected for low end applications and / or EVs (Figure 3). Its characteristics involve a capacity of 70 Ah and a cold cranking amp (CCA) of 565 A for 30s at -20°C (945 A at 25°C). In comparison to state-of-the-art 12V Pb-A batteries with L3 format, this prototype can save up to 50% in weight and 20% in volume.

The employed cylindrical sodium-ion cells provided by HiNa in 32140 format are characterized by an energy density of 130 Wh/kg, a high power up to 10C discharge peak, a long cycle life with 97 % capacity retention after 950 cycles at 1C full cycle, SoC 0-100% range, and temperature performance from -40°C to 60°C in discharge and -20°C to 70°C in charge. In addition, the cell voltage is monotonously decreasing with SoC in an almost linear manner (c.f. Figure 1). The SoC evaluation and control of the cell and thus of our 12V SIB prototype is easy, accurate and cost-efficient. Last but not least, the employed HiNa cells are safe with great resilience against excessive discharge, mechanical abuse, low atmospheric pressure and heating, in agreement with the GB/T31485 norm.

Figure 3: Images of the IAV's 12 V SIB prototypes in L3 (left) and L5 (right) formats.

The developed 12 V SIB prototypes are robust even in the worst cases scenarios. An abuse test with fast discharge cycles until full discharge has shown no significant issue. The test procedure involved resting the battery for 30 min, followed by a discharge at 600 A (8.6 C) and a 5-minute rest. This sequence was repeated until the voltage reached ≤ 6.0 V, which corresponds to 1.5 V at cell level, i.e. to an over-discharge of 1.0 V beyond the minimum operative voltage. The test was repeated with three different prototypes, yielding with the same results (Figure 4). Note 60°C is not considered at risk for the used SIB cells due to they comply with safety heating performance test at 130°C during 30 min.

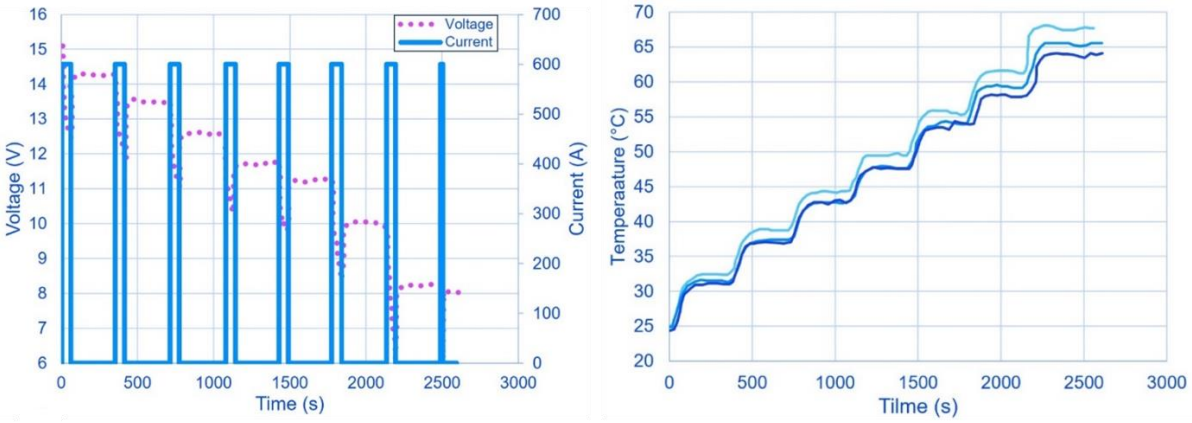

Figure 4: Abuse test with fast discharge cycles performed with three 12V SIB prototypes. Note the thermal sensor was directly located on the top of the 12 V SIBs.

The 12 V SIB prototype (Figure 5) is characterized by an efficiency similar to the one of the Pb-A battery in a real case scenario representing start of a diesel-powered ICE vehicle, with both batteries showing a voltage drop of approximately 4.3 V. In addition, the 12 V SIB has the advantage of having a voltage level significantly superior to 12.0 V at high SoC levels, with a maximum of 15.8 V being achieved. Thus, the current discharge needed to start an ICE can be significantly reduced with the 12 V SIB prototype compared to the values of the original 12 V Pb-A-based battery. The recorded difference is about 12.5 % in favor of the 12V SIB, Figure 5.

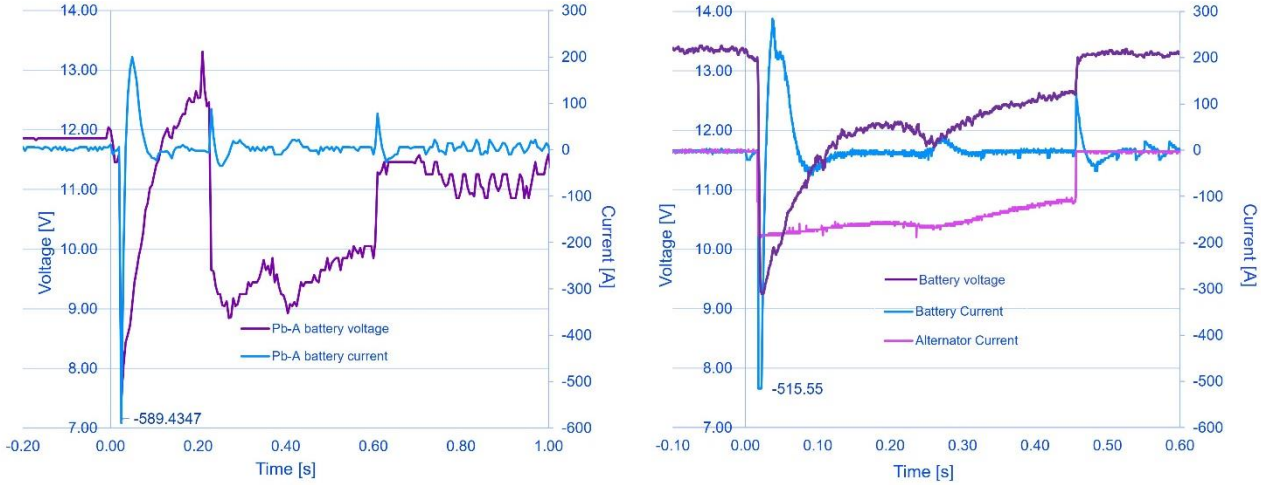

Figure 5: Real-world ICE start tests in a Peugeot 308 HDI with the original 12 V Pb-A battery (left) and the L3 12 V SIB prototype (right) including an indication of the peak discharge current, tests been performed at 20°C.

In parallel, a high-end application 12 V SIB prototype was developed with a 10P4S configuration, employing the same cells. The L5 format battery weighs 13.5 kg with a capacity of 100 Ah and a CCA power of 850 A (Figure 3). The performance and durability of the L5 prototype have been confirmed by high continuous and peak current loads at both room temperature and cold-chamber conditions at -20°C.

2.2 48 V Sodium-Ion Concept

Based on the experience and work on the 12 V battery design, we were encouraged to explore a 48 V battery architecture utilizing the HiNa SIB cells. Here, the battery pack layout is especially driven by the requirements on the battery system in terms of electrical, thermal and safety performance. Based on the identified requirements, a concept design was developed as discussed in the following sections.

2.2.1 Battery System Requirements

Because of the specifics of the mild hybrid application, a 48 V concept has to fulfill a unique set of requirements. As can be inferred from section 1.2, the type of hybrid architecture used for the hybrid drivetrain is a strong driver of the requirements of the corresponding 48 V battery system. As the P2 architecture is the current state of the art in mild hybrid electric vehicles, we decided to design a 48 V SIB battery system tailored to the requirements of this hybrid architecture. Depending on the size and design of the vehicle platform, a wide range of battery sizes may be used for the P2 architecture. In terms of energy content, net energy capacities from below 1 kWh to around 10 kWh can be considered common. With smaller designs being more space- and cost-efficient and hence tailored to passenger car applications, we decided to stay at the lower end of the aforementioned range.

To derive operational requirements, a mission profile is employed based on a roller dyno measurement performed with a P2 mHEV with a lithium-ion battery with approximately 1 kWh of energy capacity. The considered representative drive cycles involve both city and highway driving, as shown in Figure 6 for an ambient temperature of 35 °C. It is evident that the battery is frequently charged (positive current) and discharged (negative current) in a very dynamic manner. The recorded current spikes peak at around 500 A in either direction, equivalent to a current rate exceeding 20 C.

Apart from recuperation and acceleration support, the 48V battery system is expected to be employed as primary energy source for high-power auxiliary systems, such as active anti rollbars or steer-by-wire. Numerous complementary internal combustion engine technologies that have been gaining relevance lately require the implementation of a 48V system as well. For example, electric compressors and turbochargers or

electric catalysts, are associated with loads peaking at 7-8 kW and durations of up to 10 s for active exhaust gas aftertreatment component heating, yielding less than 10 C.

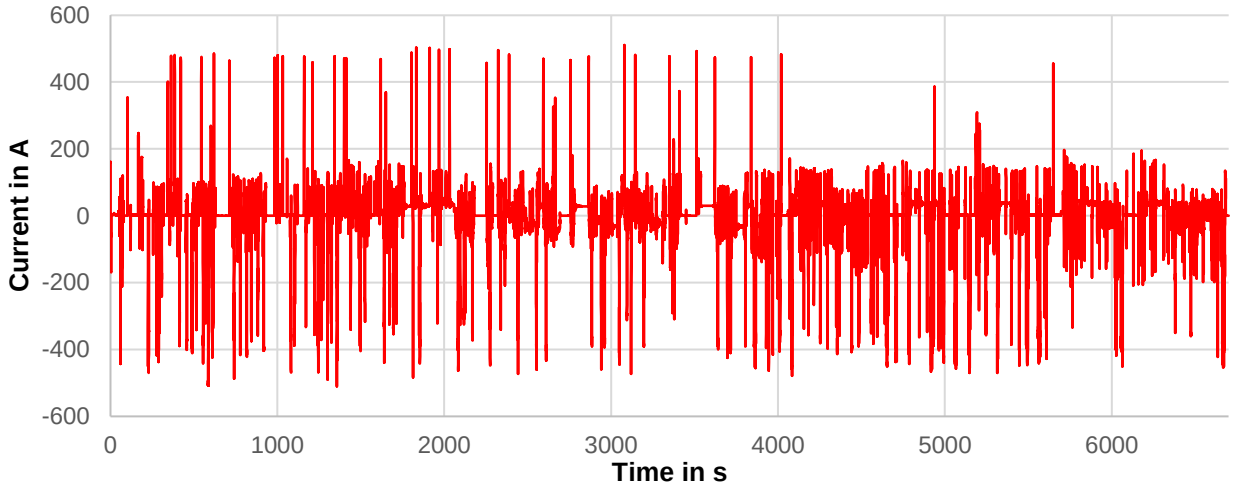

Figure 6: “Hot” 48 V battery mission profile representative for a P2 mHEV with a lithium-ion battery at 35°C ambient temperature.

The highly dynamic mission profile with comparably high peak currents, together with the requirement for non-serviceability typically posed to 48 V energy storage systems, significantly restrict the electrochemically accessible SOC range of the battery pack. This is motivated by the fact that high concentration overpotentials must be overcome to drive these currents, especially in extreme SOC ranges. Therefore, the accessible energy capacity for the specific use-case is comparably low, with capacity utilization factors of less than 60%. This constraint also defines the system voltage limits, which are tied to the accessible SOC range at a given cell configuration. Furthermore, due to the frequently applied high overpotentials, heat generation is drastically increased compared to the 12 V use case of the starter battery design. This in turn necessitates a dedicated thermal management system for the 48 V battery system.

To assess the thermal management needs of the 48 V SIB pack, a 1D model of the target 48 V battery pack design is setup, including representations of all relevant components such as cells, holders, busbars and thermal interface materials. The description of cell behavior is verified with dynamic cell data provided by the supplier. In a first step, thermal management layouts based on air and liquid cooling were compared for the drive cycle mentioned before (see Figure 7). The figure displays the hottest average cell temperatures for a hot scenario with 35°C ambient temperature. It is evident that especially in the latter part of the cycle (highway driving), large amounts of heat are released, translating to an increased cell temperature. Using an air-cooled pack results in significantly increased cell temperatures with unfavorably high temperature peaks (depending on the fan speed), compared to a liquid cooling scenario using a water-ethylene glycol mixture. For the air-cooling scenario, peaks reached nearly 55 and 45°C for high and maximum fan speeds, respectively, with both levels considered not feasible because of the corresponding impact on cell longevity. In the case of the liquid cooling approach, peak temperatures of 41 and 37°C were estimated for cooling medium inlet temperatures of 30 and 25°C at a constant coolant volumetric flow. Furthermore, Figure 6 shows that the temperature variation within the cell is more homogeneous for the liquid cooling approach. Based on these results, despite the implications in terms of costs and system complexity, an active liquid cooling approach is considered necessary for the 48 V SIB and has hence been implemented, as discussed in the following section.

The effort in terms of safety performance required for mHEV battery designs and homologation is nearly equivalent to HV batteries in BEV, with the exception of isolation resistance detection and external charge management. In this context, several categories must be addressed. Environmental tests are necessary to assess factors such as temperature shock, vibration, mechanical integrity, and water tightness. Safety tests include thermal propagation, external short circuit, and overcharge assessments. Performance and durability tests are essential to evaluate thermal performance and cycle life. Additionally, EMC tests must be conducted, along with homologation R100 requirements, such as fire resistance tests and TP alerts, necessitating the use of dedicated venting channels and seals as well as propagation mitigation measures.

The thermal runaway (TR) behavior of sodium-ion cells is linked to the specific cathode material employed within the cell, mirroring the dependency observed in lithium-ion batteries (LIBs). The severity of TR behavior follows a descending order from transition metal oxides to phosphates, pyrophosphates, and fluorophosphates.

Metallocyanide-based cathode materials, despite their limited heat release, are deemed critical due to their potential for toxic gas emissions, notably hydrogen cyanide and dicyanide. In comparison to ternary transition metal oxide cathodes utilized in LIBs, the ternary metal oxides incorporated in SIBs demonstrate a less severe TR behavior, a conclusion supported by various publications alongside our own empirical studies [13]. For the SIB cathode chemistry of the employed cells, it is anticipated that the cell will exhibit a more thermally stable behavior than that of NMC-based LIBs, thereby necessitating reduced thermal propagation mitigation measure complexity.

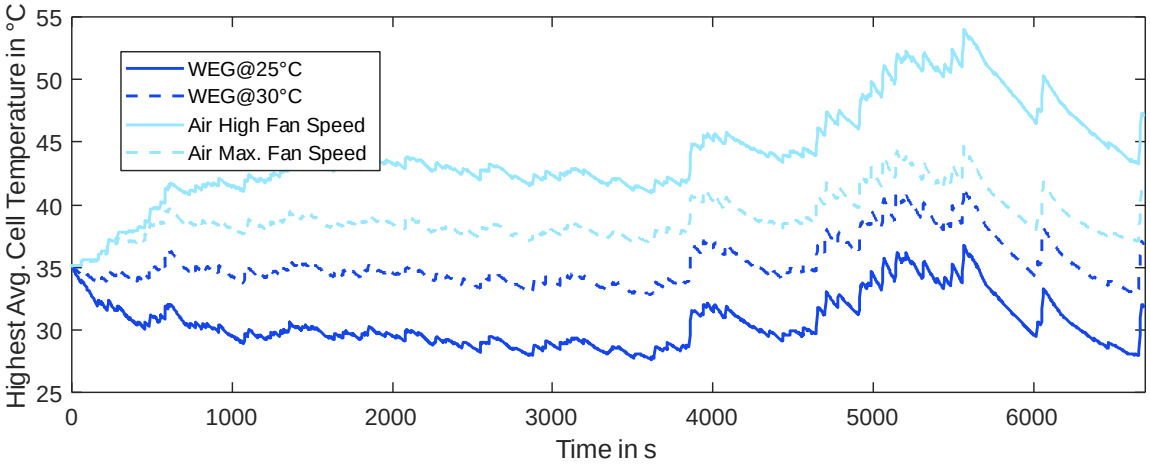

Figure 7: Highest average cell temperature in 48 V SIB modules employing different cooling layouts in hot mission profile (25°C coolant inlet, 35°C ambient).

2.2.2 **48 V Concept Design**

The final 48 V SIB battery pack concept design has been elaborated to match the requirements discussed in the preceding section. Based on the cell specification sheet, a configuration of 14 cells connected in series to meet the required voltage specifications and three cells in parallel to satisfy the continuous and especially peak current specifications well exceeding 500 A was chosen. While increasing the number of cells in parallel could further enhance current capacity, it would result in an undesirable increase in volume. Therefore, the optimal configuration consists of a total of 42 cells, arranged in two banks of 21 cells, as visible in Figure 8, yielding an overall pack capacity of 1.26 kWh.

The final concept design incorporates cells standing upright, secured by top and bottom cell holders, ensuring stability and efficient use of space, as shown in Figure 8. The cells are organized into two banks, each consisting of an arrangement of three by seven cells, to maintain minimal deviation from a squared casing layout for maximized rigidity given the 14s3p configuration. Due to the cells being opposite-terminal cells, this arrangement includes alternating cell orientations to facilitate serial connections with minimal bus bar lengths, optimizing electrical pathways. To further enhance performance, the bus bars connecting the two banks, along with the socket leads, have increased thickness to reduce resistive losses. The alternating orientation requires venting into two voids located at the top and bottom. These are connected to venting channels implemented in the cell holders, thus prohibiting the contact of the hot venting gases with the cells, and are combined into a single volume at one end of the battery casing, featuring a burst membrane for in-pack pressure management, Figure 8.

As established in the previous section, the employed design incorporates liquid cooling as the preferred method over air cooling, enhancing thermal management efficiency. As depicted in Figure 8, a cooling ribbon is placed on every other cell row in the longitudinal direction, ensuring effective heat dissipation across the battery and minimized temperature gradients. While being less complex and more cost-efficient, the implementation of a simple (bottom) plate cooling is not feasible because of the opposite-terminal layout of the employed sodium-ion cells. The battery management system board, along with electrical and fluidic connectors, are located at the front end of the battery casing, thus eliminating the prospective for any venting gas contact.

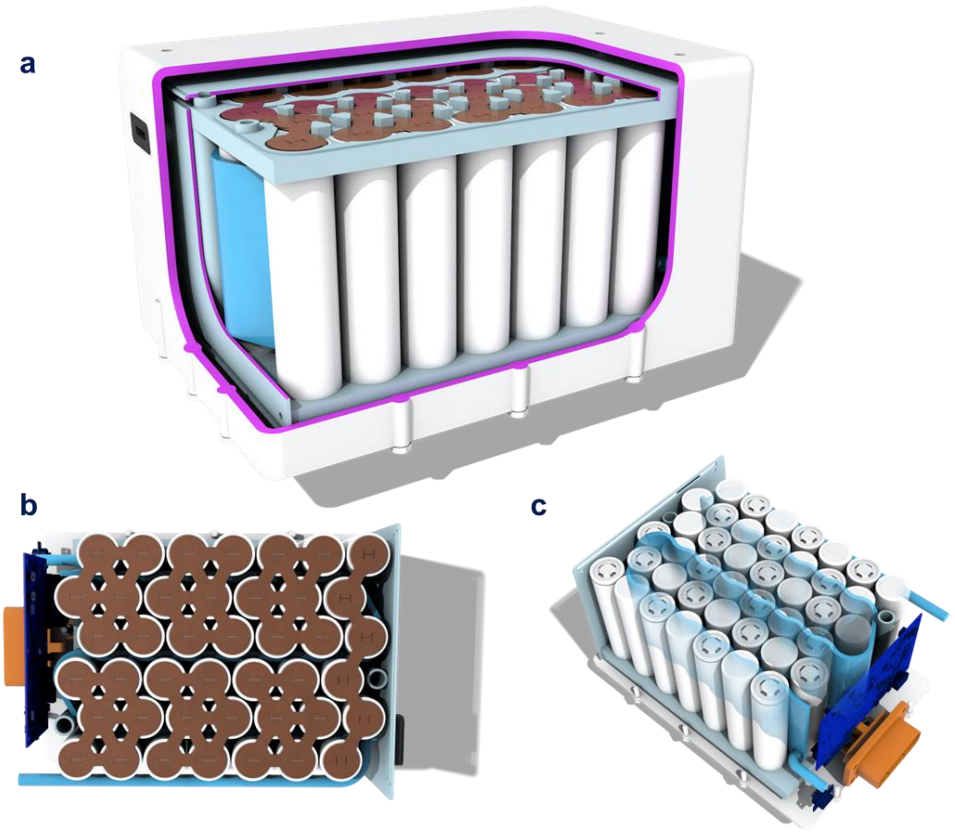

Figure 8: Overview of IAV's 48 V SIB module concept design.

2.2.3 Thermal Performance of the Concept Design

The thermal performance of the final pack design was evaluated the one-dimensional modeling methodology employed for the requirement assessment, with the integration of a liquid cooling strategy tailored to the selected design for thermal management. As can be seen in Figure 9, the battery SoC undergoes a gradual discharge throughout the drive cycle, starting at 80%.

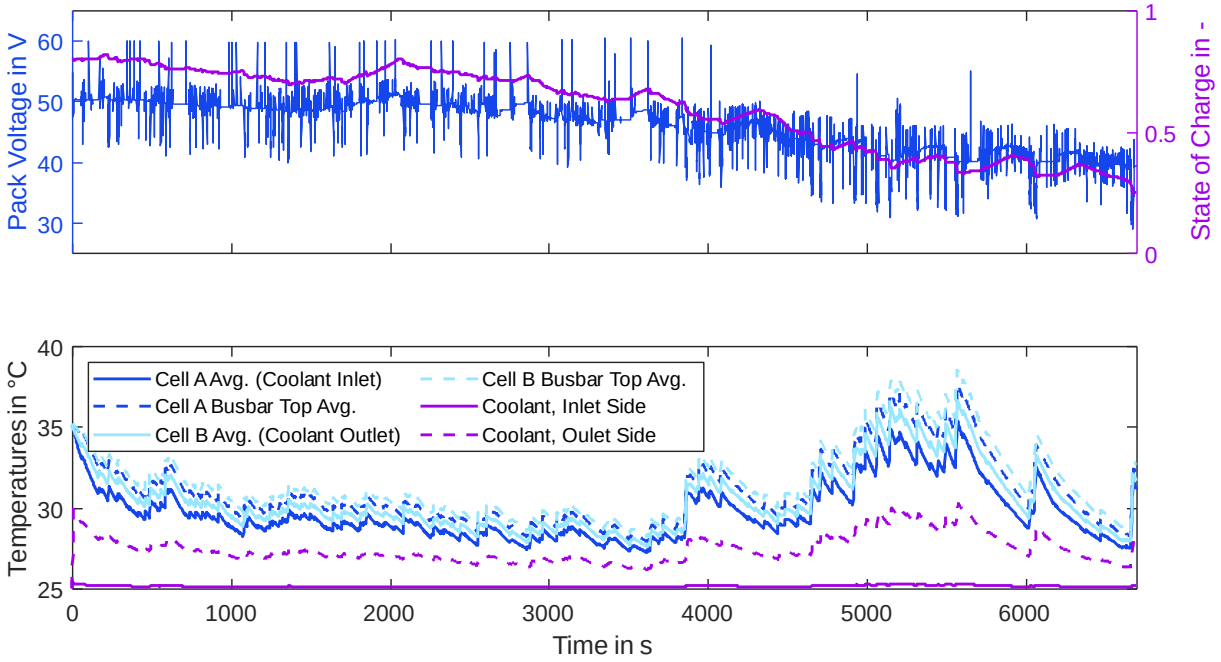

Figure 9: 48 V SIB module (14s3p configuration) performance and main component temperatures with active water-ethylene-glycol cooling in hot mission profile (25°C coolant inlet, 35°C ambient).

During city driving, the operation remains balanced, resulting in a relatively stable SoC profile, whereas highway operation induces a more pronounced discharge. From a component temperature perspective, the cell temperatures are characterized by marginal differences between the coolant inlet and outlet, indicating a good temperature homogeneity within the pack. The bus bar temperatures are elevated due to the additional resistive losses inherent within the bus bars. Despite the consideration of a thermally demanding mission profile characterized by an ambient temperature of 35°C and a constant coolant volumetric coolant flow of 1 l/min, neither the bus bar nor the battery cell temperatures approach critical thresholds. This outcome substantiates the reasonable selection of component dimensions, affirming their adequacy in terms of thermal performance. The design choices ensure that the thermal management system can effectively maintain operational integrity and efficiency, even under challenging environmental conditions, thereby validating the robustness of the cooling approach and the overall system architecture.

3 Comparative study LFP vs. SIB

3.1 Study Design

The comparative study presented in this section focuses on cylindrical 32140 SIB cells as employed in IAV's 12 V and 48 V battery concepts presented in the previous section, which incorporate a ternary transition metal oxide-based cathode and soft carbon anode. These cells are optimized for high energy capacity, with all data regarding the key performance indicators (KPIs) provided by the cell supplier. In addition to the selected SIB cells, a screening process was conducted to identify further comparable candidates, emphasizing low cost and sustainability characteristics. Lithium-ion batteries with LFP cathode chemistry, currently the dominating newcomer on the low voltage battery market, were identified as meeting the necessary metrics. The comparison between SIB and LFP cell chemistries encompasses performance as well as economic and sustainability comparisons.

Specific data for LFP cell **KPIs**, particularly current maps for charge and discharge, is not readily available as a single dataset for high-energy cells of the used format. Consequently, we decided to derive these data from a parametrized coupled electrochemical-thermal model (EPCM), which is validated through literature comparison with available literature data for LFP cells. The simulation environment employs a pseudo 2D (P2D) modeling approach for the electrochemical processes characterizing each cell chemistry, coupled with a 3D temperature (2D-axisymmetric) model of a single cylindrical cell. This modeling approach offers the advantage of providing various parameters that can be adapted for different cell design optimizations, such as high power and high energy designs. Parameter gradients within a battery cell play a crucial role for the cell's dynamic voltage or current response, where high-power cells differentiate from high-density cells. Thus, the discretization over the cell thickness and the additional intra-particle dimension offered by P2D models, solving the charge and mass balance equations in the electrodes and electrolyte phases, allows to consider the discussed parameter gradients and hence the dynamic cell behavior. Accordingly, investigations regarding cell design parameters can be performed for optimizing the cell for one target application. The primary modeling result is the generation of time-current-temperature maps for both charge and discharge, based on three criteria: maximum or minimum cut-off voltages, maximum desired operating temperature, and negative electrode potential to account for the risk of plating formation. Plating is anticipated to occur, particularly for combinations of higher C-rates, lower temperatures, and high state of charge, even if the operating SoC window is reduced, which accelerates cell aging. These time-based maps are generated through an automated iterative process using a Nelder-Mead algorithm-based optimizer.
Supply chain and cost assessments within this study are solely derived from existing literature sources, which provide a comprehensive dataset for LIBs in general as well as LFP chemistries. However, the data available for SIBs is notably limited, and often lacks comparability to the specific ternary transition metal oxide cathode chemistry selected for this study. Thus, we evaluated SIBs as a general category, without differentiating chemical composition variations among SIB cathodes, leading to a generalized understanding of SIB economics. Furthermore, it must be remarked that the SIB cannot benefit from the same production scaling effects.

To compare the sustainability aspects of the considered SIB cells with LFP cells, we conducted an **LCA analysis** of the cells comprising four phases. For novel battery technologies and cell chemistries, the LCA methodology assesses potential environmental impacts based on differences in electrode active materials, thus

aiding in battery concept definition. In the study performed in this contribution, the system boundary is set at the battery cell production (Cradle-to-Gate), as use-phase and end-of-life impacts largely depend on the electricity mix and recycling processes, rather than the technology itself. Furthermore, the possible scenarios for subsequent use of the battery are diverse and complex. In contrast, there are criteria such as cycle life and the use of secondary materials from a recycling loop that are technology-dependent and can be of importance along the further life cycle. The manufacturing phase reflects the technology's impact by being influenced by materials, energy density, processes, and cell design. The functional unit for the LCA study is defined by the battery cell excluding its peripherals, with the outer boundary defined up to the cell housing. The reference flow is one kilowatt-hour (kWh) of energy, also used as normalization unit. The impact assessment uses characterization factors/models from Leiden University (CML 2001 - Aug. 2016) and USEtox (2.12) [28]. Five of the European Commission's 16 recognized impact categories for environmental footprint (EF) are considered, with these being the Global Warming Potential (GWP), Acidification Potential (AP), Abiotic Depletion Potential (ADP elements), Human Toxicity Potential cancer (HTP), and Ecotoxicity Potential (ETP) [29]. These categories offer a holistic view of product system sustainability, highlighting shifts in environmental impacts resulting from technological changes. Dedicated databases (Sphera LCA for Experts Version 10.9.0.31, Content Version 2023.2) provide the basis for assessing cell production impacts [31]. Masses and chemical compositions are sourced from the cell and battery design process. The modelling is performed by adopting a conservative approach, treating waste and scrap via the cut-off approach without credits. Resulting gaps are filled with literature data to ensure sufficient quality. The analysis reflects current standards, with cell production in Europe using the European electricity mix.

3.2 Key Performance Indicators (KPIs)

Table 1 compares typical values for key performance indicators of SIB and LFP cells. While most SIB cells available today are optimized for high energy density, their typical power density is comparable to that of high-power LFP cells. The performance of SIBs is dependent on the specific chemistry employed, section 1.3, and like in the case of LFP, a SIB cell can be designed either energy- or power-oriented. Thus, the KPIs of SIBs listed in Table 1 can appear broad at first look. The development of SIB technology and market is expected to lead to an optimization of the different SIB designs for the desired target applications.

KPI	Sodium-ion	Lithium iron phosphate - High energy	Lithium iron phosphate - High power
Gravimetric energy density [Wh/kg]	100-175	160-205	70-100
Gravimetric power density [W/kg]	3,000+	1,600+	2,200-3,500
Cycle life (80% BoL; 80% DoD)	4,000+	3,000+	6,000+
Peak C rate (2 sec. @ 25°C)	24-100+	8.5	60
Low temperature performance	Good to Moderate	Moderate	Moderate
Safety performance [13]	Good to Moderate	Good	Good

Table 1: High-level KPI comparison for SIB, high-energy LFP and high-power LFP cells.

3.2.1 Energy density

The current energy density of SIBs typically ranges from 100 to over 170 Wh/kg at the cell level, with CATL recently unveiling a SIB with an energy density of 175 Wh/kg [4, 7]. Some next-generation models announced by suppliers, including CATL and Faradion, are anticipated to exceed 190 Wh/kg. This is slightly lower than the energy density of LFP energy-type cells but higher than LFP power-type cells. Typically, LFP energy cells have a specific energy of around 160 Wh/kg, with high-end models reaching up to 205 Wh/kg, such as the recently announced Shenxing CATL. On the other hand, LFP power-type cells have a lower energy density

compared to today's state-of-the-art SIB, with values ranging from 70 to 90 Wh/kg, as these cells are optimized for very rapid charging and discharging, as well as high cycle life.

3.2.2 **Power**

SIBs offer the advantage of high-power capability, even in the case of cells optimized for energy density. Generally, SIBs provide higher power density compared to energy-type LFP cells, but they are comparable to or slightly lower than power-type LFP cells. Specifically, sodium-ion cells have reported power densities around 1 kW/kg, with the potential to exceed 3.5 kW/kg [7]. This is significantly higher than typical energy-type LFP cells, with specific power densities in the region of 200 W/kg, but also somewhat lower compared to power-type LFP cells, which can reach up to 425 W/kg or more, depending on their design. Advanced sodium-ion cells however may rival or even surpass power-type LFP cells in terms of power delivery capabilities.

3.2.3 **Low Temperatures and Lifespan**

SIBs are generally characterized by high capacity retention, potentially maintaining over 96% retention after 3,850 cycles. A lifespan with 80% State of Health exceeding 25,000 cycles can be anticipated, depending on the cathode chemistry [9]. It is well known that the energy and power of LFPs significantly decrease at cold temperatures, as also shown in Figure 10 for the cell considered in this study, aligning with academic research [O]. In contrast, SIBs demonstrate more resilient performance, capable of charging at temperatures as low as -20°C and retaining up to 82% capacity at -30°C [9].

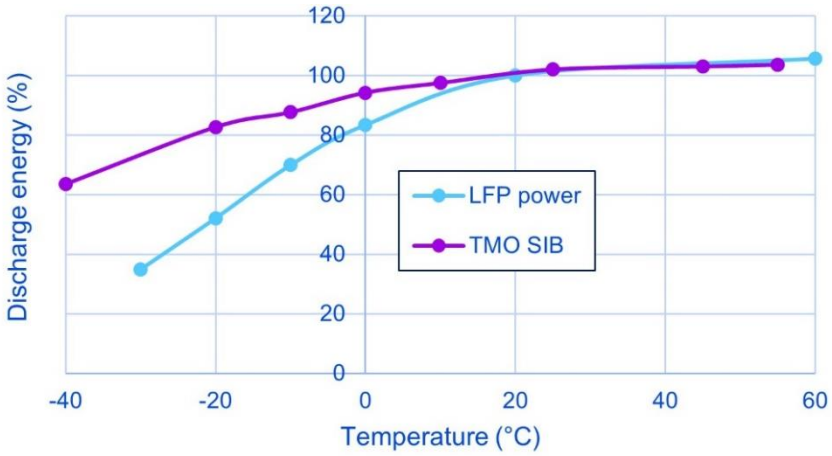

Figure 10: Discharge energy at different temperatures for the considered transition metal SIB and LFP power cells at 1 C, reference represented by oxide SIB capacity at 20°C (=100%).

3.2.4 **Integration**

When comparing the thermal management needs for high-power applications between sodium-ion and LFP batteries, several important differences appear. Sodium-ion batteries usually perform better in cold conditions and can operate and charge at negative temperatures while LFP batteries typically charge only down to 0°C. This means sodium-ion batteries often do not need active heating systems in cold environments, making thermal management easier in such conditions. They also have lower internal resistance and better ionic conductivity at low temperatures, helping them maintain performance without producing too much heat.

On the other hand, LFP batteries, especially those made for high current output, produce a lot of heat during heavy use. This makes strong thermal management systems necessary to prevent overheating, loss of capacity, and faster aging. Cooling methods like advanced liquid cooling are often needed to keep cell temperatures even and to protect safety and lifespan in high-power LFP battery packs. LFP cells also have a narrower ideal temperature range and are more sensitive to performance loss when temperatures are too low, as ion movement inside the battery becomes slower.

Although less sensitive than LFP batteries, sodium-ion batteries show also changes in resistance and impedance depending on temperature, especially when they are at a low state of charge. Because of this, careful management of both temperature and charge level is needed to keep them efficient and long-lasting. However, sodium-ion batteries generally have better thermal stability and a safer design, which reduces the risk of thermal runaway compared to some types of lithium-ion batteries, making thermal management somewhat

easier. Last but not least, SIB has more sloped open circuit voltage curves than LFP making accurate estimation of the State of Charge easier.

In the next step, the evaluated chemistries are assessed in the perspective of a 48 V application for a mild hybrid powertrain, as detailed for the 48 V SIB concept design presented in the previous section. The final design of the 48 V battery pack is directly influenced by the type of cell and chemistry used, as summarized in Table 2. Due to their respective voltage ranges (see Figure 1), fewer SIB cells are required in series compared to LFP cells to meet the pack voltage requirements. On the other hand, the peak power requirements impact the necessary number of parallel connections. Consequently, configurations of 17p2 and 14p3s are identified as the optimal compromise for the SIB and LFP chemistries respectively. The resulting 48 V SIB pack is positioned between the 48 V LFP high-energy and LFP high-power options in terms of weight, power, and energy. While power and weight are critical for targeted mHEV applications, limited energy capacity can accelerate cell aging and reduce overall energy recuperation, thus diminishing CO_2 reduction potential. It is important to note that the discharge power performance of batteries typically decreases with the State of Charge; the lower the SoC, the lower the maximum discharge power. Additionally, for mHEV applications, the SoC operating window should be restricted to 30% - 90%, defined at a target operating temperature of 25°C based on best practices. Detailed optimization in this context can be achieved by incorporating aging mechanisms into the respective models, for example in the process of developing the battery management system functions.

48 V Pack parameters	**Sodium-on**	**Lithium iron phosphate - High energy**	**Lithium iron phosphate - High power**
Number of cells	42	34	34
Configuration	14p3s	17p2s	17p2s
Approx. total cell weight [kg]	11.2	12.3	8.2
Approx. total cell volume [L]	7.3	5.9	5.9
Discharge peak power (2 sec. @ 25°C) [kW]	30.8	22.6	38.4
Discharge peak power (2 sec. @ 0°C) [kW]	25.6	0.9	19.0
Gross Energy [kWh]	1.26	1.61	0.71

Table 2: Comparison of SIB, high-energy LFP and high-power LFP cell-based 48 V battery pack parameters for a mHEV application.

Overall, the SIB pack is approximately 3 kg heavier than the equivalent LFP power cell-based one, offering approximately 20% less maximum power at 25°C, but more than 77% higher energy content. Additionally, as previously noted, SIBs demonstrate significantly more robust performance at cold temperatures compared to LFPs. At 0°C, the discharge peak power of the 48 V SIB decreases by approximately 17% compared to its performance at 25°C, whereas the power of LFP power cell-based pack drops by about 50%. The discharge peak power of the SIB at 0°C is approximately 34% greater than that of the 48 V LFP power cell.

While our 48 V battery concept design includes active thermal management for the pack, which could counteract low-temperature effects, several arguments support the importance of considering the impact of low temperatures on the pack performance impacts. Firstly, 0°C is not uncommon in many regions worldwide, and no temperature management system offers instantaneous efficiency; there is always a latency period, even in small batteries, and the worst-case scenario must be considered in pack design for safety reasons. In addition, temperature heterogeneities are inevitable with a ribbon cooling design, and the temperature gradient is expected to have a lower negative impact on the electrical performance and durability of the 48 V SIB compared to the 48 V LFP. In this context, heterogeneous temperatures within an active cell led to more heterogeneous electrochemistry, promoting mechanical and electrochemical degradation.

3.3 Supply Chain, Sovereignty and Cost

The value chain for lithium iron phosphate cell manufacturing is largely dominated by the influence of one country, this being China, with the notable exception of lithium mining, where approximately 75% of the lithium raw material is sourced from Chile or Australia. Despite this geographical limitation, China exerts substantial control over the successive stages of the value chain, including refining, cathode and anode material production, and cell manufacturing. Notably, around 90% of the cathode active material for LFP cells is produced within China, underscoring its dominance in this sector. This strategic advantage is further bolstered by China's approach to mitigating its geographical disadvantage in lithium raw material distribution through full ownership of mining enterprises at sourcing locations or through joint ventures with incumbent operators. For SIBs, China maintains a dominant position in terms of cell production capacity, although key market players are located in Europe. The abundance of sodium, which is approximately three orders of magnitude higher than that of lithium, coupled with its more homogeneous geographical distribution within the lithosphere, renders sodium raw material sourcing more economically viable due to decreased costs associated with material transport. Furthermore, SIBs do not require copper foil as a negative current collector, which further reduces production costs.

However, watt-hour-normalized costs for SIBs currently remain higher than those for LFP batteries, attributable to several factors. The production of hard carbon often used in SIB anodes (although not in the case of the sodium-ion cell considered in this study) is more expensive than the soft carbon used in LIBs due to purification and electricity demands [32]. Additionally, SIB production cannot currently benefit from the same maturity of supply chains as LIBs, which drives up costs. The production scale of SIBs remains limited compared to LIBs, meaning that economic scaling effects do not apply equally. Furthermore, due to the lower energy density of SIBs, fixed costs for cell manufacturing are higher when assessed on an energy capacity-based metric. Nevertheless, with increased maturity of both technology and production scale, significant cost savings compared to LIBs are anticipated, with estimates suggesting around 30% savings compared to LFP batteries. However, as economic parity is likely to be reached in the mid-2030s, costs are currently only expected to be advantageous from the late 2040s onwards using baseline considerations [33].

3.4 Sustainability

Studies have indicated that Lead Acid (Pb-A) based batteries, while still dominating the 12 V market as discussed in the introduction section, is characterized by a higher environmental impact compared to the lithium-ion-based formulations gaining on relevance for low-voltage applications [34]. The life cycle assessment performed in this study further reveals a clear advantage in terms of environmental impact for the sodium-ion based cell, which is characterized by more than 60% lower normalized environmental impact compared to its LFP counterpart based on the Environmental Footprint 3.1 methodology, Figure 11. This ratio in environmental impact is not expected to change in the near future, indicated by the values estimated for 2030.

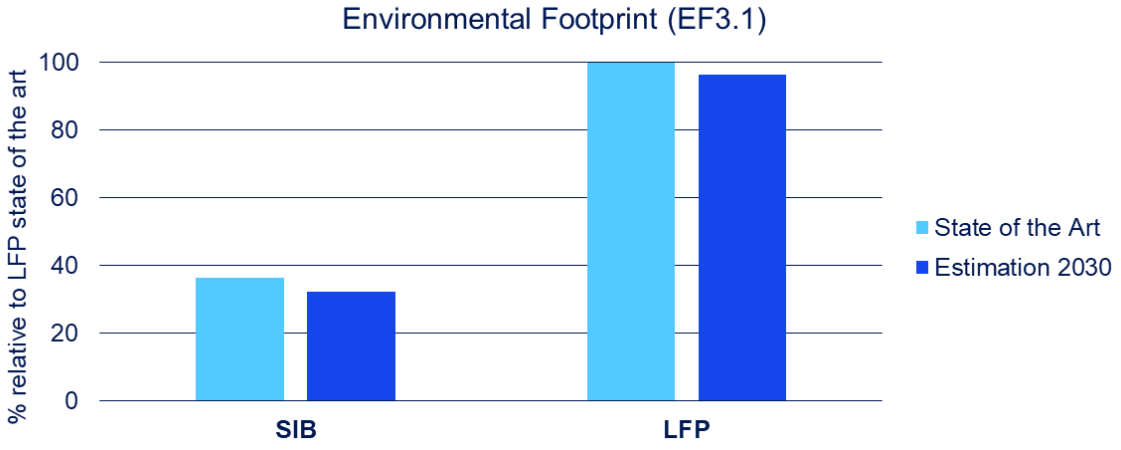

Figure 11: Normalized total environmental footprint of LFP and SIB cells based on state-of-the-art and estimated for 2030. Values calculated according to the Environmental Footprint methodology (EF3.1) based on five impact categories, state-of-the-art LFP used as reference (= 100%).

Multiple impact categories must be considered when comparing technologies, with changes in battery cell design and especially chemistry typically resulting in significant shifts in impact categories. This motivates the calculation of an overall sustainability score based on established methodologies, as performed above for EF3.1. The overall normalized result shown in Figure 11 hence reflects five impact categories in total, with the respective values in the single categories shown in Figure 12 for the considered LFP and SIB cells. The SIB has the lowest values in the AP, ADP elements, HTP, and ETP categories and nearly equal GWP per kWh.

GWP values for SIB vary due to active materials, manufacturing processes, and production region [40]. For cylindrical sodium-ion cell production, similar processes to conventional cylindrical LIB cells can be assumed [31]. Established processes handle more material, increasing time and energy consumption. The cathode active material (Fe, Cu, Mn mixed oxides), is represented using literature data. Layered oxides, the largest mass component, are conservatively estimated, with energy requirements sourced from literature. Soft carbon is considered for the anode, being inexpensive and easy to produce.

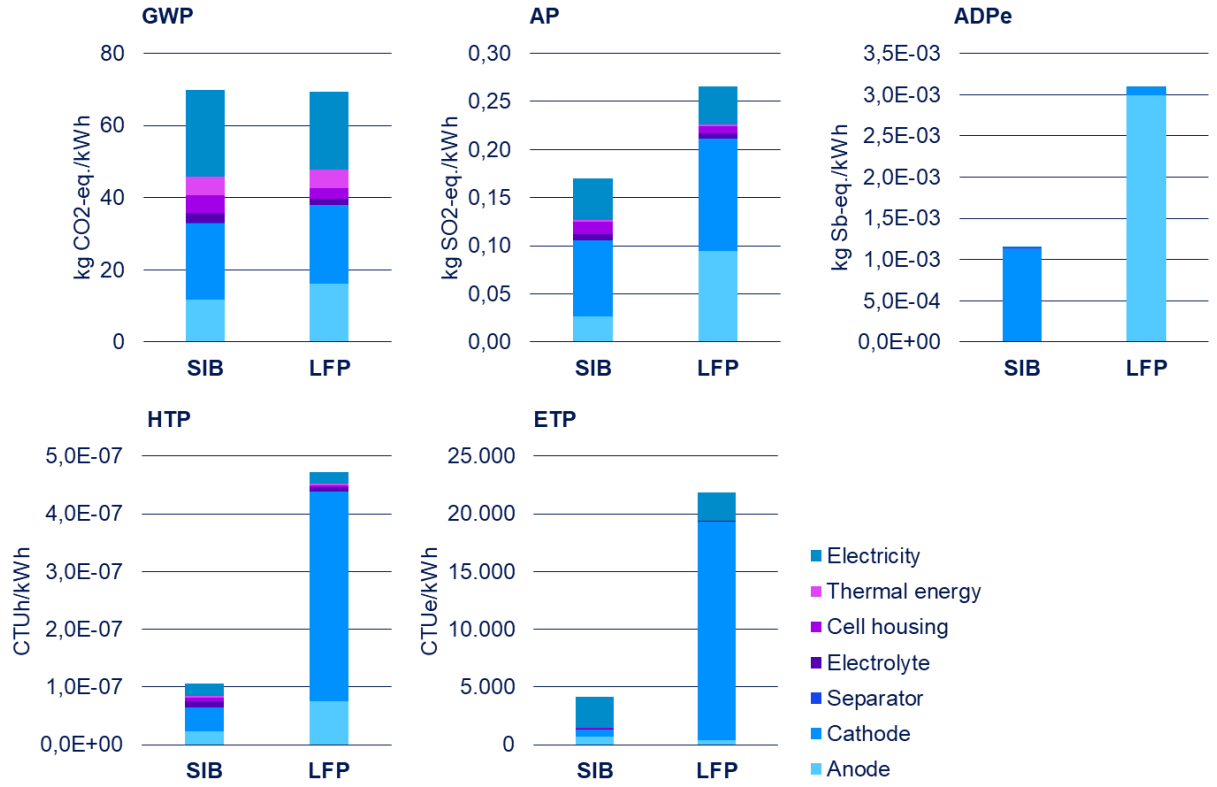

Figure 12: Global Warming Potential (GWP), Acidification Potential (AP), Abiotic Depletion Potential (ADP) elements, Human Toxicity Potential cancer (HTP) and Ecotoxicity Potential (ETP) per kWh from cell production for the considered state-of-the-art SIB and LFP battery cells.

Based on these assumptions, the considered SIB and LFP cells have similar GWP per kWh, with normalized values of approximately 70 kg CO_2-eq./kWh, Figure 12. The SIB benefits from less CO_2-intensive anode material that is however counterbalanced by heavier cell housing, more electrolyte and higher electricity consumption. Cathode and thermal energy are very similar for the SIB and LFP batteries. In the AP category, the SIB impact is decreased by approximately 33% in comparison to the LFP cell. The main reason is the anode, where the impact of the SIB is 25% of the LFP's. The cathode is the second largest contributor to the SIB's lower impact in the AP category, with AP factor values of approximately 0.8 kg SO_2-eq/kWh, which is ca. 40% lower than the AP impact of the LFP cathode at 0.115 kg SO_2-eq/kWh. For ADP, the LFP cell's copper anode foil is a hotspot, accounting for ~93% of the ADPe value per kWh, while the SIB uses only aluminum foil for both the anode and cathode current collectors. The SIB cathode contains transition metal (Cu, Mn) representing 90% of its ADPe value, which still is less than 40% of the ADPe of the LFP.
HTP of the SIB represents 22% of the LFP's. In the former, the cathode is the main contributor but remains still inferior to 50% of SIB's total HTP value. The contributions of the anode and electricity seem almost identical. The composition of HTP contributors of the LFP cell is very different. Its cathode contributes more than 75% of the total HTP value per kWh. The second largest contributor, the anode, reaches 17% of the LFP's total HTP.

The difference between the SIB and LFP is even higher for the ETP factor, with the former being characterized by less than 20 % of the latter's ETP value. Electricity counts for ca. 70 % of the total ETP of the SIB. Also in this category, the cathode is the hotspot for the LFP with more than 80 % of its total ETP, while electricity is only the second largest contributor, accounting for only approximately 15% of the LFP's total ETP.
Thus, SIB technology is favored for its sustainability and comparably low environmental impact over various lithium-ion batteries [10], including lithium iron phosphate as clearly demonstrated in this study. SIBs thus have significant potential for vehicle concepts in terms of sustainability, with industrialization anticipated to further reduce corresponding emissions.

3.5 LFP vs. SIB for Low-voltage Applications: Summary

Figure 13 summarizes the study results by comparing the KPIs of different cell chemistries in the context of a 12 V application. We observe that the use of Pb-A, as a reference, market-dominating technology, is mainly driven by its competitive price and ease of integration related to its very safe chemistry. Nonetheless, considering the potential for a future ban because of the high toxicity, these advantages are expected to ultimately lose significance. Present-day alternatives, such as LIB LFP and NMC, stand out as clear replacements, especially given the availability and scalability of these chemistries. A closer look at the potential of SIB suggests it could become an interesting alternative, especially in terms of sustainability, performance, and even future price competitiveness.

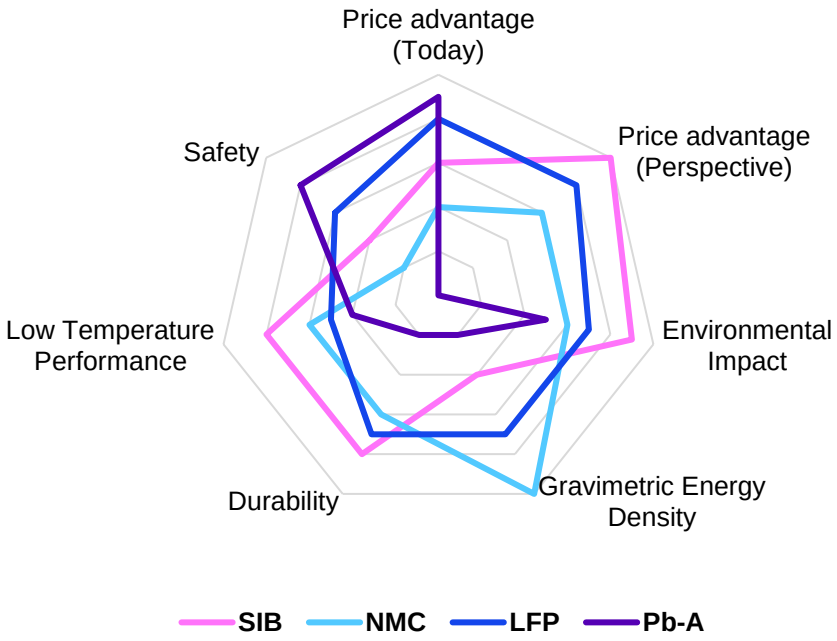

Figure 13: Comparison of different cell chemistries focusing on 12V applications, with Pb-A currently dominating the market.

For the 48 V application, the comparison of key KPIs shown in Figure 14 focuses on the main chemistry candidates considered in this study, namely LFP (both power- and energy-type) and SIB, as an alternative to NMC-based battery modules. Although SIB is not currently the best candidate in terms of price, it is expected to become the cheapest chemistry in the future as scalability and production increase, based on BOM and market projections. It also demonstrates good performance at low temperatures and offers strong sustainability benefits. While it may not be best-in-class in other categories, the performance gaps are relatively small, making this chemistry a strong trade-off option when considering all evaluated factors together.

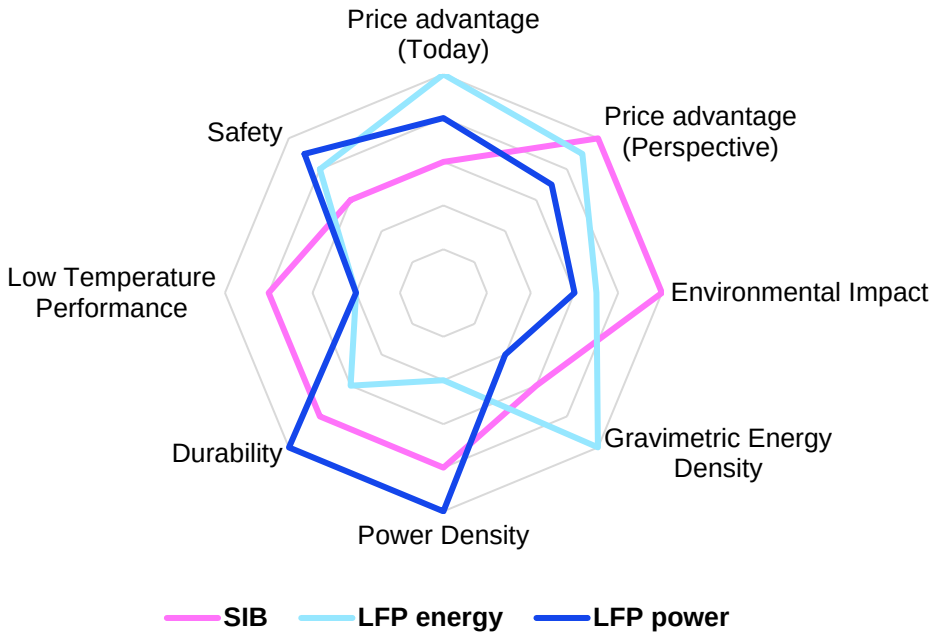

Figure 14: Comparison of different cell chemistries focusing on 48 V applications.

4 Conclusions and Outlook

Based on IAV's dedicated 12 V SIB prototype and 48 V SIB concept designs, the study on the potential of SIBs for low-voltage mobility presented in this contribution highlights several important findings and future implications for low-voltage battery technology. Sodium-ion batteries represent a promising alternative to the typically used lead-acid (12 V) and lithium-ion batteries, mainly because of their robustness, highly abundant raw materials, high durability, good performance and potential lower cost in the future.

In addition to its excellent safety features, being fully resistant to overcharge, over-discharge, and short-circuit conditions, the SIB benefits from a lower environmental impact compared to its competitors especially thanks to it not containing lead or lithium. Based on the results from the performed study, significant improvements in key environmental indicators such as global warming and acidification potentials can be expected by 2030, manifesting SIBs as a sustainable electrochemical energy storage solution also for future applications. Performance tests across different temperatures show that SIBs deliver stable discharge energy, which is important for reliable high-power operation in various climates, as typical for low-voltage applications.

In conclusion, this study indicates that sodium-ion batteries do not represent a miraculous solution, as they do not excel in comparison to other technologies across most categories. However, their characterization as a "jack of all trades, master of none" positions them as a potential transformative force in low-voltage mobility, offering a sustainable, safe, and cost-effective alternative to the battery technologies currently dominating the market. The implementation of SIBs can lead to significant advancements in the design and performance of low-voltage systems, with further development and scaling of the SIB technology expected to support its widespread adoption within the automotive industry, ultimately contributing to a more environmentally friendly and sustainable future.

Acknowledgments

The authors thank HiNa Battery Technology Co., Ltd for their support of this study and their collaboration in the development of the 12V Sodium-Ion Battery (SIB) prototype. Furthermore, the presented work could only be conducted thanks to the collaboration of many domain-specific specialists, with the number of parties involved going beyond the authors list. In this respect, the authors would like to express their sincere thanks to all colleagues involved and in particular Manfred Prüger and Chatham David McLaughlin.

References

[1] EU regulation of the European Parliament and of the council 2023/851 approved on 19/04/2023 “Strengthening the CO2 emission performance standards for new passenger cars and new light commercial vehicles in line with the Union’s increase climate ambition.

[2] Euro news on 19/09/2024 https://www.euronews.com/business/2024/09/19/eu-car-industry-calls-for-urgent-action-as-ev-new-car-sales-tumble, accessed on 17/04/2025.

[3] Bauknecht S. et al. Comparing the Cold-Cranking Performance of Lead-Acid and Lithium Iron Phosphate Batteries at Temperatures below 0 ◦C, Batteries, ISSN 2313-0105, 9 (2023), 176.

[4] Volta foundation, Battery report 2023, https://volta.foundation/download-the-2023-battery-report, accessed on 17/04/2025.

[5] Tian, X., Guo, R., Bai, Y., Li, N., Wang, X., Wang, J., Wu, C., High-Performance High-Nickel Multi-Element Cathode Materials for Lithium-Ion Batteries. Batteries 2023, 9, 319.

[6] Energy Storage news, https://www.energy-storage.news/first-half-world-largest-200mwh-sodium-ion-project-comes-online-china/, assed on 17/04/2025.

[7] Tarascon J.-M., J, Na-ion versus Li-ion Batteries: Complementarity Rather than Competitiveness, Joule, ISSN 2542-4351, 4 (2020), 1613-1620.

[8] Tapia-Ruiz N. et al. 2021 roadmap for sodium-ion batteries, Journal of Physical Energy, ISSN 2515-7655, 3 (2021), 031503.

[9] Battery Design from chemistry to pack https://www.batterydesign.net/hina-nacr32140-mp10/ accessed on 17/04/2025

[10] M. Sens et al., Toward a sustainable vehicle concept, part 1: The high-voltage battery – technologies and methods, 44th International Vienna Motor Symposium, 2023.

[11] Zhang, P., et al., An Overview of Different Approaches for Battery Lifetime Prediction, IOP Conf. Ser.: Mater. Sci. Eng., 199, 012134, 2017.

[12] Geoffrey J. May, Alistair Davidson, Boris Monahov, Lead batteries for utility energy storage: A review, Journal of Energy Storage, Volume 15, 2018, Pages 145-157.

[13] Sallard S, Nolte O, von Roemer L, Soltani B, Fandakov A, Mueller K, Kalogirou M, Sens M. Exploring Thermal Runaway: Role of Battery Chemistry and Testing Methodology. World Electric Vehicle Journal. 2025; 16(3):153.

[14] Yuliya Preger et al ., Degradation of Commercial Lithium-Ion Cells as a Function of Chemistry and Cycling Conditions, J. Electrochem. Soc., 167, 120532, 2020.

[15] Startpower Lithium Operatin Instructions, https://cs-batteries.de/mediafiles/Anleitungen/ZM-CSX12125-1500A-D-E.pdf, accessed on 15/03/2025.

[16] EAS Batteries HP601300 LFP 22 data sheet, https://eas-batteries.com/system/files/attachments/Data%20sheet%20HP601300%20LFP%2022%20Ah%20rev.4.6.pdf, accessed on 17/03/2025

[17] Volta foundation, Battery report 2024, https://volta.foundation/battery-report-2024, accessed on 17/04/2025.

[18] Toshiba high-power cells,https://www.global.toshiba/ww/products-solutions/battery/scib/product-next/product/cell/high-power.html, accessed on 17/04/2025.

[19] Sun, B., Qi, X, Song, D., Ruan, H., Review of Low-Temperature Performance, Modeling and Heating for Lithium-Ion Batteries, Energies, 2023; 16(20):7142.

[20] T. Richard Jow et al., Factors Limiting Li+ Charge Transfer Kinetics in LiIon Batteries, J. Electrochem. Soc., 165, A361, 2018.

[21] Liao, L, Zuo, P., Ma, Y. et al., Effects of temperature on charge/discharge behaviors of LiFePO4

cathode for Li-ion batteries, Electrochimica Acta, Volume 60, 2012, Pages 269-273, ISSN 0013-4686.

[22] Belgibayeva, A., Rakhmetova, A., Rakhatkyzy, M., et al., Lithium-ion batteries for low-temperature applications: Limiting factors and solutions, Journal of Power Sources, Volume 557, 2023, 232550, ISSN 0378-7753.

[23] Zhu, G., Wu, O., Wang, Q., Kang, J., Wang, J.V., The Modeling and SOC Estimation of a LiFePO4 Battery Considering the Relaxation and Overshoot of Polarization Voltage, Batteries, 2023; 9(7):369.

[24] Mukai, K., Inoue, T., Kato, Y., Shirai, S., Superior Low-Temperature Power and Cycle Performances of Na-Ion Battery over Li-Ion Battery, ACS Omega 2017 2 (3), 864-872.

[25] CarNewsChina on 18.11.2024, CATL announces second-generation sodium battery, normal discharge at -40°C, https://carnewschina.com/2024/11/18/catl-announces-second-generation-sodium-battery-normal-discharge-at-40c/, last accessed on 02.02.2025.

[26] Gao, Y., et al., A 30-year overview of sodium-ion batteries, Wiley, Carbon Energy. 2024;6:e464.

[27] Bhutia PT, Grugeon S, El Mejdoubi A, Laruelle S, Marlair G. Safety Aspects of Sodium-Ion Batteries: Prospective Analysis from First Generation Towards More Advanced Systems. Batteries. 2024; 10(10):370. https://doi.org/10.3390/batteries10100370

[28] Leiden University, "CML-IA Characterisation Factors," Database, Department of Industrial Ecology, 2016: https://www.universiteitleiden.nl/en/research/research-output/science/cml-ia-characterisation-factors, last accessed on 15.02.2023.

[29] Fantke, P., Bijster, M., Guignard, C., Hauschild, M., Huijbregts, M., Jolliet, O., Kounina, A., Magaud, V., Margni, M., McKone, T.E., Posthuma, L., Rosenbaum, R.K., van de Meent, D., van Zelm, R., "USEtox (corrective release 2.12)," 2019: https://usetox.org/model/download/usetox2.12, last accessed on 02.02.2025.

[30] The Advanced Rechargeable & Lithium Batteries Association, "PEFCR - Product Environmental Footprint, Category Rules for High Specific Energy Rechargeable Batteries for Mobile Applications," Report, 2020.

[31] Sphera Solutions, Inc., "Life Cycle Assessment Software (GaBi),": https://sphera.com/life-cycle-assessment-lca-software/, last accessed on 31.01. 2025.

[32] Yuxin Liu, Techno-economic Analysis of Biomass Conversion to Hard Carbon Materials, Thesis, KTH Royal Institute of Technology, Stockholm, Sweden.

[33] Yao, A., Benson, S.M. & Chueh, W.C. Critically assessing sodium-ion technology roadmaps and scenarios for techno-economic competitiveness against lithium-ion batteries. Nat Energy 10, 404–416 (2025).

[34] Ryutaka Yudhistira, Dilip Khatiwada, Fernando Sanchez, A comparative life cycle assessment of lithium-ion and lead-acid batteries for grid energy storage, Journal of Cleaner Production, Volume 358, 2022, 131999, ISSN 0959-6526.

[35] Peters, J., Baumann, M., Binder, J., Weil, M., „On the environmental competitiveness of sodiumion batteries under a full life cycle perspective – a cell-chemistry specific modelling approach," Sustainable Energy Fuels, 5, 6414, 2021.

Presenter Biography

During his already more than two decades with IAV, Karsten Mueller has collected exhaustive experience as a developer and manager. He holds a degree in Systems Theory and has been responsible in different positions along the whole bandwidth of electrics and electronics applications in the automotive environment since 2008. His stations also comprise management positions at IAV China and IAV India. Since 2022, Karsten has been Senior Vice President Electrified Systems with a strong focus on battery development.